11.98 ± 1.27 mg per gram of liver, compared with 11.55 ± 1.26 in five control rabbits. The nitrogen content of cytoplasm in the treated rabbits was 11.23 ± 0.64 mg per gram of liver, compared with 10.63 ± 0.39 in the controls.

Table 2 shows that the increase in nitrogen and phosphorus found in the smooth membrane fraction after drug treatment corresponds to the increase in protein content, phospholipid phosphorus and soluble phosphorus-containing compounds. There also was a smaller rise in the RNA content. A large increase in cytochrome b_5 (Table 1) was found in the smooth membrane fraction.

These results are in accord with the experiments of Gelboin and Sokoloff who showed that previous treatment of rats with phenobarbital stimulated the incorporation of amino acids into microsomal proteins of cell-free liver preparations (*8*).

The increase in smooth membranes (approximately twofold) was associated with an even higher increase in activities of enzymes found in smooth membranes and involved in drug metabolism (two- to sixfold). Changes in the amount of activity of the enzymes that hydrolyze procaine (*9*) reduce the nitro group of chloramphenicol (*10*), demethylate monomethylaminoantipyrine (MAAP) (*11*), and oxidize hexobarbital (*11*), eunarcon (*12*), and $NADPH_2$ (*13*) are shown in Table 1. The smaller increase in enzyme activity of rough membranes after treatment with phenobarbital must be partially due to incomplete separation of smooth and rough membranes and is probably not significant. Fouts (*7*), in a study of the distribution of drug-metabolizing enzymes between rough and smooth membrane fragments, observed much smaller relative values in the rough membranes than those that are reported here.

Activities of three enzymes found in the endoplasmic reticulum, but not involved in drug metabolism were also examined (Table 1). There was a small increase in the rate of hydrolysis of glucose-6-phosphate (*14*) as a result of drug treatment. Activities of NADP-nucleosidase (*15*) and adenosine triphosphatase (*14*) did not change. Variations in the age and strains of the rabbits may account for some of the range of values obtained in identical experiments.

The three-fold rise in the amount of cytochrome b_5, determined by direct measurement of the soret band (*16*); the parallel increase in cytochrome-*c*-reductase activity (*17*); and the increased rate of procaine hydrolysis, probably provide the best evidence for a real multiplication of enzymes.

The combined morphological and biochemical observations indicate a nonspecific adaptation to injections of a drug. Besides phenobarbital, other drugs with high lipid solubility, such as tolbutamide and nikethamide, produce the liver changes described above. The result is to decrease the duration of action and effectiveness of a number of drugs metabolized to less effective or inactive compounds (*4*). Barbiturates, but not alkaloids, belong to the group of drugs producing these changes. Tolerance, developed with repeated use of barbiturates, but not morphine and other narcotic compounds, can be explained as a result of induction of enzymes produced by the drug itself (*18*, *19*).

H. REMMER
H. J. MERKER

Department of Pharmacology and
Institute for Electronmicroscopy,
Freien Universität,
Berlin-Dahlem, Germany

References and Notes

1. H. Remmer, *Arch. Exptl. Pathol. Pharmakol.* **237**, 296 (1959); *Metabolic Factors Controlling Duration of Drug Action*, B. B. Brodie, Ed., vol. 6 of the *Proceedings of the 1st International Pharmacological Meeting* (Pergamon, New York, 1963), p. 235; F. G. Brazda and R. W. Baucum, *Federation Proc.* **19**, 137 (1960); R. Kato, *Experientia* **16**, 9 (1960).
2. A. H. Conney, C. Davidson, R. Gastel, B. B. Burns, *J. Pharmacol. Exptl. Therap.* **130**, 1 (1960).
3. A. H. Conney, E. C. Miller, J. A. Miller, *J. Biol. Chem.* **228**, 753 (1957).
4. H. Remmer and H. J. Merker, *Klin. Wochschr.* **41**, 276 (1963).
5. K. R. Porter and C. Bruni, *Cancer Res.* **19**, 997 (1960).
6. G. E. Palade and P. Siekevitz, *J. Biophys. Biochem. Cytol.* **2**, 171 (1956).
7. J. R. Fouts, *Biochem. Biophys. Res. Commun.* **6**, 373 (1961).
8. H. V. Gelboin and L. Sokoloff, *Science* **134**, 611 (1961).
9. Incubated at *p*H 8.8; the decrease in optical density was determined at 315 mμ.
10. J. R. Fouts and B. B. Brodie, *J. Pharmacol. Exptl. Therap.* **119**, 197 (1957).
11. H. Remmer, *Arch. Exptl. Pathol. Pharmakol.* **235**, 279 (1959).
12. 5-Isopropyl-5-β-bromoallyl-*N*-methylbarbituric acid. Determined by the method used for hexobarbital (*11*).
13. Incubated at *p*H 7.4; the decrease in optical density was determined at 340 mμ.
14. Glucose-6-phosphate incubated at *p*H 6.5; ATP incubated at *p*H 7.4 with $MgCl_2$; inorganic phosphate determined: C. H. Fiske and Y. Subbarow, *J. Biol. Chem.* **66**, 375 (1925).
15. S. P. Colowick, N. O. Kaplan, M. M. Ciotti, *ibid.* **191**, 447 (1951).
16. D. Garfinkel, *Arch. Biochem. Biophys.* **71**, 100 (1957).
17. Unpublished results.
18. H. Remmer, *Ciba Found. Symp. Drugs Enzymes* (1962), p. 276.
19. Supported by the "Deutsche Forschungsgemeinschaft." The assistance of Mrs. Reich and Miss Deyhle is gratefully acknowledged.

16 October 1963

Polyribosomes: Size in Normal and Polio-Infected HeLa Cells

Abstract. *HeLa cells normally contain a distribution of polysome sizes, and the largest polysomes contain over 40 ribosomes. After infection with polio virus and actinomycin-D treatment, a new class of polio-induced polysomes are found, some of which contain up to 60 ribosomes. Examinaton of these polysomes suggests a mechanism for protein synthesis with this polycistronic RNA.*

Polyribosomes or polysomes are clusters of ribosomes held together by RNA. These rather than the single ribosomes are the active units for protein synthesis in vivo (*1–3*). Polysomes were first characterized in electron-microscope studies on extracts from the rabbit reticulocyte which manufactures the single protein hemoglobin (*1*). The polysomes so obtained consisted of groups of four, five, or six ribosomes which could be seen, in shadowed preparations, as tightly clustered groups or, in stained preparations, as extended ribosomal arrays. In these initial observations, the narrow distribution of polysome size was attributed to the fact that the reticulocyte was manufacturing a single protein, since the ribosomes were thought to be held together by the messenger RNA which contains the information in nucleotide sequence necessary for synthesizing the protein.

In cells, such as the mammalian HeLa cells, which are manufacturing a large variety of proteins, sedimentation studies on a sucrose gradient (*4*) indicate a broader distribution of polysome size. Analysis of pulse-labeled RNA from the polysomes of the HeLa cell strongly suggested that the ribosomes in a polysome are simultaneously attached to a single strand of messenger RNA. This interpretation was reinforced by finding a new species of polysomes in cells infected with polio virus which have been treated with actinomycin D (*4*). This antibiotic inhibits the endogenous production of messenger RNA but does not adversely affect the production of viral RNA. These new polysomes appear larger in the sucrose-gradient analysis and they are associated with the production of polio-virus specific protein (*5*). We now present the results of an electron microscope study of the polysomes in both the normal HeLa cell and in the HeLa cell which has been infected by polio virus.

Polysomes were isolated from extracts of the cytoplasm (*4*) of HeLa cells in the log phase of their growth. The cells were incubated for 1 minute with C^{14} amino acids (30μc per 10^9 cells) to label the nascent protein, and then they were homogenized (*6*) and treated with 0.5 percent sodium deoxycholate. The extract was placed on a sucrose gradient and various components were separated by ultracentrifugation [25,000 rev/min (*6*) for 60 min] in a swinging-bucket rotor. After centrifugation, the bottom of the tubes was punctured to remove the contents. The optical density of the material at 2600 Å was read directly in a recording apparatus and fractions were collected for measuring the radioactivity and for examination in the electron microscope. The results of this analysis are shown in Fig. 1, in which the material is sedimenting toward the left. The peak at 74*S* is associated with single ribosomes. Sedimenting more rapidly is a broad distribution of material. At the maximum optical density the sedimentation constant is near 200*S*, although the range extends beyond 300*S* at its furthest limits. For electron microscope examination, small samples were taken from various tubes along the gradient and placed on an electron microscope grid coated with silicon monoxide. The microscope grid was washed with gradually decreasing concentrations of sucrose and buffer (0.01*M* KCl, 0.0015*M* $MgCl_2$, 0.01*M* tris buffer, *p*H 7.4) and then finally with distilled water; it was dried in air. The material was shadowed with platinum at an angle of 5 : 1 and then examined in an electron microscope (*6*) at 16,000 ×. A number of grids were made from each fraction and several fields were scanned. The number of ribosomes in each cluster was counted and related to the position along the gradient (Fig. 1). The 74*S* peak is composed of single ribosomes. The optical-density peak of the polysome distribution consists largely of clusters containing five or six ribosomes. These clusters are thus similar in size to those found in the polysomes from the reticulocyte. Polysomes which sediment further down the gradient contain a much larger number of ribosomes in each cluster.

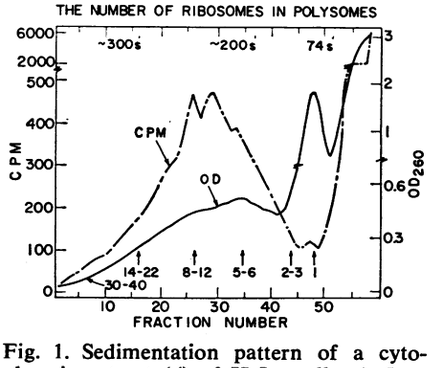

Fig. 1. Sedimentation pattern of a cytoplasmic extract (*4*) of HeLa cells. A 5 to 20 percent sucrose gradient was used. The vertical arrows indicate the fractions examined in the electron microscope. The associated numbers indicate the number of ribosomes found in polysomal clusters. Single ribosomes have a sedimentation constant of 74*S* and approximate sedimentation constants are listed for other points on the gradient.

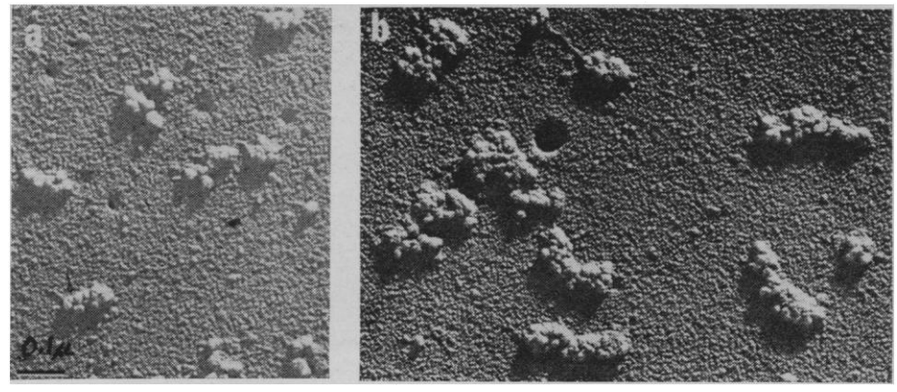

Fig. 2. Electron micrographs of HeLa polysomes. (*a*) Fraction 34 (Fig. 1). (*b*) Larger polysomes obtained from fraction 16. The close clustering is a common feature seen with larger polysomes and is probably a drying artifact.

Figure 2*a* shows a portion of the electron microscope field from fraction 34 (Fig. 1) which occurs near the peak of the optical-density curve. These polysomes appear quite similar to the air-dried, platinum-shadowed polysomes obtained from reticulocytes. They are characteristically clustered, and appear to be in contact in shadowed preparations; however, negative- and positive-stained preparations from reticulocytes show that there is an interribosomal gap of 50 Å to 150 Å (*1*, *7*). Figure 2*b* shows an electron miscroscope field taken from fraction 16 (Fig. 1) further down the gradient. Here the ribosomes appear to be clustered, forming a dense and compact area. In such very large clusters it is often difficult to make an accurate count of the number of ribosomes since they are not clearly delineated. It should be emphasized that this is the appearance of the polysome as seen on the electron microscope grid and is probably not the form which occurs in the intact cell. Air drying does tend to produce an artifical clumping, possibly causing the longer polysomes to be clustered. Two lines of evidence support such a view. In some fields, clumping is incomplete, and large polysomes are seen as extended, essentially linear structures. In addition, thin sections of tissues prepared for electron microscopy frequently show long strings of ribosomes rather than the clustered grouping shown in Fig. 2*b*.

The number of ribosomes in various

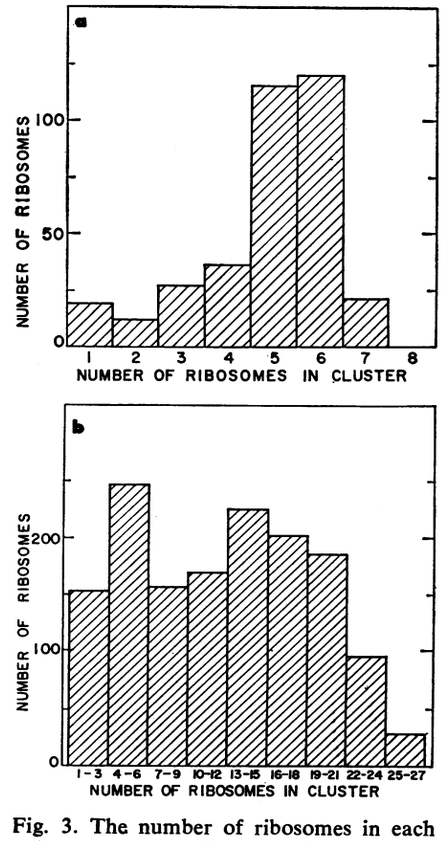

Fig. 3. The number of ribosomes in each polysomal cluster for two different positions on the gradient in Fig. 1. (*a*) The distribution in fraction 34. Clusters of five and six ribosomes predominate here, and the smaller fractions are breakdown products. (*b*) The distribution of polysome sizes in fraction 16. The large number of smaller polysomes is an indication of the fragility of the larger polysomes.

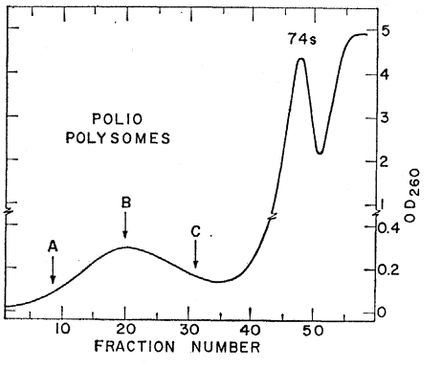

Fig. 4. A sedimentation pattern of cytoplasmic extract from polio infected HeLa cells. A sucrose density-gradient sedimentation similar to that described for Fig. 1 was used except that a 15 to 30 percent sucrose gradient was used, and the centrifugation time was 90 min. Fractions at *A*, *B*, and *C* were examined in the electron microscope.

fractions was determined by making statistical counts in several electron microscope fields. Fraction 48 (Fig. 1) consisted of single ribosomes, and fraction 43 had predominantly clusters of two and three. The results for fraction 34 at the optical density maximum are shown in a histogram (Fig. 3*a*). There is a predominance of clusters containing five to six ribosomes. The units containing one, two, or three ribosomes probably are breakdown products associated with the manipulation necessary for preparing the sample. Otherwise they would not have sedimented at this place in the gradient. Since the polysome consists of a string of ribosomes held together by an RNA strand, it is not surprising that they show this degree of fragility, which was also seen in the reticulocyte preparations (*1*). Breakdown of the sample is even more evident when larger polysomes with a higher sedimentation coefficent are examined.

Figure 3*b* shows the distribution obtained from electron microscope fields of fraction 16 (Fig. 1). There is a continuum of polysome sizes, with some slight peaking in the range 14 to 22 ribosomes. Again polysomes containing one to nine ribosomes would probably not be found this far down the gradient. Their presence in this distribution results from the fragmentation of larger polysomes containing approximately 14 to 22 ribosomes. The borderline of this assumed distribution is somewhat arbitrary, so that the numbers shown in Fig. 1 are approximate in the leading edge of the distribution. It is extremely difficult to get a reliable indication of the size distribution of larger polysomes because of the degradation of the sample associated with manipulation.

The size range of polysomes includes 30 to 40 ribosomes (fraction 7, Fig. 1), indicating that these electron microscope fields show many polysomes in that size range, as well as some containing even more ribosomes. However, the majority of the polysomes in that fraction are smaller. It is likely that the larger polysomes are more susceptible to fragmentation because of their size.

In contrast to the specialized reticulocyte which manufactures only hemoglobin and has a narrow polysome distribution, the HeLa cell makes a large variety of proteins and has a polysomal distribution which varies continuously from small units containing two or three ribosomes up to very large clusters containing 30 to 40 ribosomes. The incorporation of C^{14}-amino acids (Fig. 1) shows that all of these classes of polysomes are active in protein synthesis since the radioactivity approximately follows the optical density of the polysomes except in the region where the single ribosomes are found. The single ribosomes have very little if any capacity to synthesize proteins, a characteristic compatible with our understanding of the mechanism of protein synthesis on polysomes (*2*, *8*). The single ribosomes are believed to initiate protein synthesis when they attach themselves to the messenger RNA which is usually part of a polysome.

During the continuous monitoring of optical density, we observed a series of maxima in the optical-density profile. In the reticulocyte polysomes (*2*) such contours are associated with single ribosomal increments in a polyribosomal series. In the HeLa preparations we can often see contours which extend out to polysomes containing eight to ten ribosomes. The optical-density results show good correlation with the electron-microscope findings. However, these contours do not go out much beyond eight or ten ribosomes which suggests that the different sizes of polysomes are no longer sharply separating in the sucrose-density gradient. In part, this results from the slow rate of change of sedimentation coefficient with increasing ribosome number for large polysomes. However, it may also be associated with the fact that the longer polysomes can assume a variety of shapes if there is less than maximum packing of ribosomes on the available messenger length. Thus the sedimentation rate of several different sizes of large polysomes may overlap appreciably.

Infection of HeLa cells with polio virus results in a gradual decrease in the number of polysomes which are seen in the cell over a period of 2 or 3 hours (*4*). This decrease in the number of polysomes in HeLa cells can also be accelerated by exposing the cells to actinomycin D which combines with DNA and inhibits the production of RNA copies from it. Thus when polio-infected cells are treated with actinomycin D, there is a marked decrease and an eventual disappearance in the number of polysomes seen in the cell over the first 2 or 3 hours after infection. This is apparently due to the additive effect of the impairment of endogenous messenger RNA production by actinomycin D as well as to a degradation of polysomes associated with polio virus infection. After 3 hours of this treatment, the extract of HeLa cells has lost all of its polysomes as judged both by optical density and amino acid incorporation.

While actinomycin D inhibits the replication of DNA viruses, it does not prevent the reproduction of small RNA viruses. Thus about 3½ hours after polio virus infection and treatment with actinomycin D, a new species of polysomes begins to appear. These polysomes are directly associated with the polio infection. They have a much larger average sedimentation constant than normal cell polysomes and have been shown to contain newly synthesized polio protein (*5*).

We have studied the polio polysomes in the electron microscopes. HeLa cells (8×10^8) were infected with type I polio virus (20 to 30 plaque-forming units per cell). The cells were treated with 5 μg of actinomycin D per milliliter for 2 hours prior to infection. Cell lysates were made 3 to 4 hours after infection and placed on the sucrose-density gradient. The results of one such analysis is shown in Fig. 4 in which the optical density is plotted. The sharp 74*S* peak due to single ribosomes can be seen, as well as a more rapidly migrating peak which has an estimated sedimentation constant somewhat over 300*S*. This is in contrast to the normal HeLa cell polysome peak which has an optical-density maximum near 200*S*. However, since the RNA

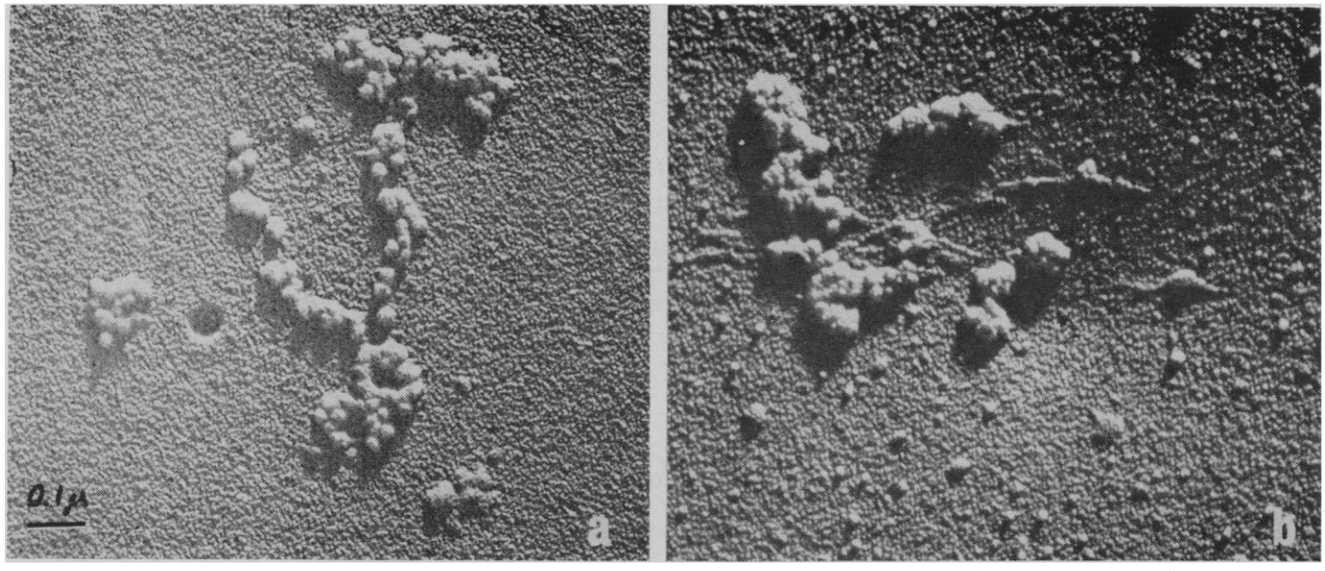

Fig. 5. Electron micrographs of polio virus induced polysomes. The specimens were obtained from fraction *A* of Fig. 4. (*a*) The large Y-shaped polysome is in an extended configuration and contains about 60 ribosomes. The compact cluster above it probably is a different polysomal fragment. (*b*) A polysomal cluster which also shows many small particles in the field. These may be viral capsid protein.

component of polio virus has a molecular weight of 2 million, we would anticipate that it might organize larger polysomes than the messenger RNA associated with uninfected HeLa cells.

We have examined the polio polysomes in three different regions on the gradient (Fig. 4). The most rapidly migrating sample was at position *A* (Fig. 4), and slower components at positions *B* and *C*. In the electron microscope, the leading edge (*A*, Fig. 4) showed very large polysomes. A variety of different configurations were seen, some producing large clustered masses of ribosomes in which 40, 50, and often 60 ribosomes were seen forming large plate-like structures. This clustering of the ribosomes is interpreted as being a drying artifact similar to that which is seen with the smaller polysomes. However, in other preparations the polysomes were more extended, showing that they were essentially linear structures. An example of an open configuration is shown in Fig. 5*a* which contains a polysome with approximately 60 ribosomes held together presumably by the same messenger RNA strand. In common with the naturally occurring polysomes, a very low concentration of ribonuclease will convert the polio polysomes into singly sedimenting ribosomes. In these polysomes the center-to-center spacing between adjacent ribosomes is approximately 300 Å to 400 Å which is similar to that seen in other polysomes.

The large size of the polysomes associated with polio virus infection is consistent with the idea that the polio virus RNA strand remains intact and has ribosomes attached along its entire length. We can estimate the number of ribosomes which would attach themselves to a fully loaded polio virus RNA strand. In the reticulocyte, the messenger RNA coding for the polypeptide chains of hemoglobin must have at least 450 nucleotides to contain the structural information for the protein (*2*). These polysomes are seen with a distribution of four, five, or six ribosomes attached to each cluster. However, polio virus RNA contains approximately 6000 nucleotides. Accordingly, one might estimate that a fully loaded RNA strand of this size should hold 50 to 70 ribosomes. The largest size of polio polysomes which is observed is consistent with the intact viral RNA strand being fully loaded with ribosomes. In addition, newly synthesized RNA has been extracted from these polysomes and has the sedimentation properties of polio RNA (*9*).

In some experiments in which samples were taken at 4 hours, the leading edge of the polio polysome distribution showed another type of particle in the electron microscope field in addition to the polysomes (Fig. 5*b*). These were small molecules which look like ellipsoids of revolution with a long axis of 70 Å, a smaller axis near 50 Å, and an estimated molecular weight of 80,000. This is approximately the molecular weight found in the capsomere of the polio virus (*10*). As mentioned previously, the polio polysomes contain material which combines with antibodies to a derivative of virus-coat

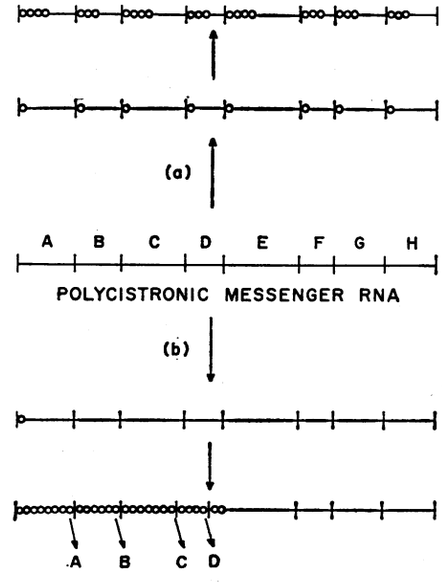

Fig. 6. Representation of two possible methods of polycistronic messenger RNA "read-out" during protein synthesis. The messenger RNA codes for eight proteins (*A* through *H*) and the small circles represent ribosomes. (*a*) The ribosomes are attached at each cistron and initiate independent synthesis of the various proteins. (*b*) There is one attachment site for the entire messenger strand, and proteins are sequentially synthesized.

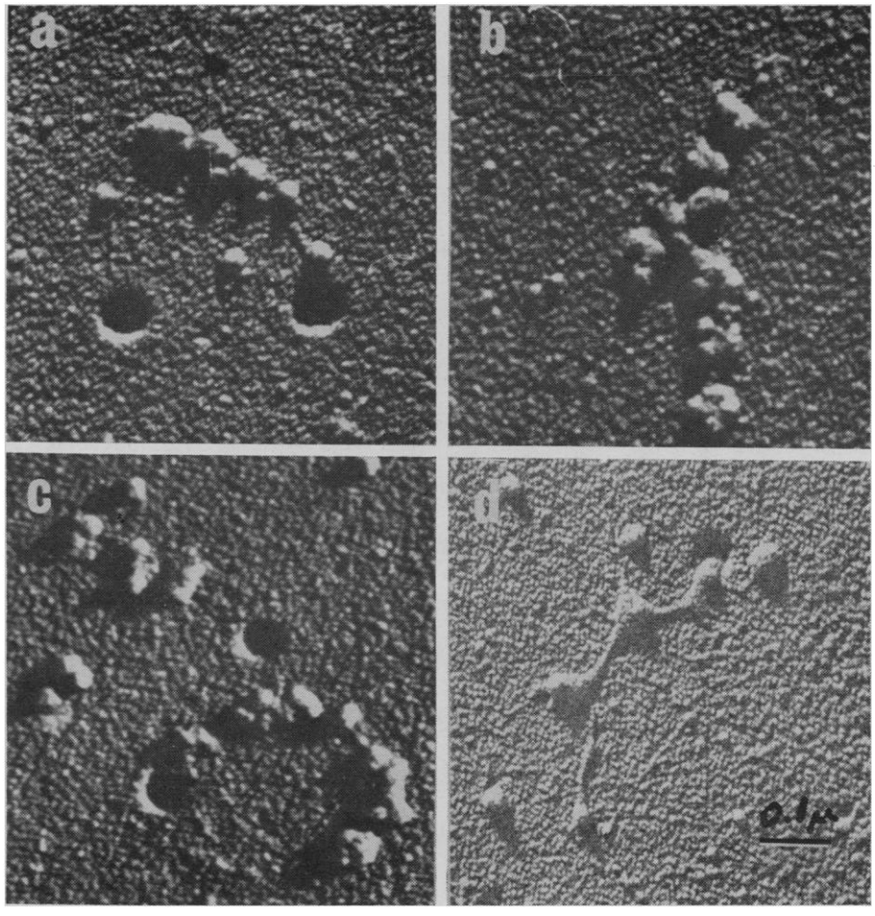

Fig. 7. Electron micrographs of polio virus induced polysomes. (*a-c*) Three different polysomal fields obtained from fraction *B*, Fig. 4. It can be seen that there are gaps in the polysomes, often 500 Å in size. (*d*) A field from fraction *C*, Fig. 4. Several ribosomes can be seen attached to a thread-like structure, with large spacings between them. This field was heavily shadowed with platinum.

protein (*5*). Thus it seems possible that some of the polio-coat protein is carried down the gradient with the polysomes. It is interesting to note that although the more rapidly sedimenting fractions at position *A* (Fig. 4) show these particles, they are not seen on the samples taken from positions *B* and *C* in the same gradient.

The entire polio virus RNA molecule appears to act as a messenger RNA inside the HeLa cell. The only well characterized proteins for which the viral RNA is almost certainly the messenger are the capsid proteins, of which there appear to be two (*11*). In addition, the virus has other functions which are likely to be associated with other proteins made by the polio virus RNA acting as a messenger. These include a new RNA polymerase activity in the cytoplasm (*12*), the specific disruption of cellular polyribosomes, and the suppression of host cell RNA synthesis. Thus, the number of proteins which polio virus RNA could code for may be five or more. Hence, we may describe the viral RNA as a "polycistronic messenger RNA."

We would like to understand the mechanism by which a polycistronic messenger RNA makes proteins. When polysomes were discovered in reticulocytes which are manufacturing a single protein molecule, it was assumed that the distribution of polysomes containing four, five, and six ribosomes was associated with a statistical attachment of ribosomes at one end of the polysome and detachment at the other end, together with detachment of the completed protein (*1*, *2*). Recent experiments on the ribosomes of HeLa cells tend to support this interpretation of polysome function (*8*). Thus we believe that a ribosome attaches itself at one end of the polysome and gradually moves along the messenger RNA strand until it reaches the end of the messenger strand where both ribosome and newly synthesized polypeptide chain are released. We would like to inquire how this mechanism would be modified by the existence of a polycistronic messenger RNA. Two alternative types of mechanisms are shown in Fig. 6. In this diagram, the polycistronic messenger RNA can make eight proteins, *A* through *H*. The lower mechanism (*b*) is one in which the polycistronic messenger strand has one attachment site. Protein synthesis begins by a ribosome attaching at the end. The ribosome begins to move along the messenger strand as the polypeptide chain grows; at the end of a particular cistron, it releases its polypeptide chain and starts to manufacture the next polypeptide chain. Thus, there is a sequential manufacture of a group of proteins. When the messenger is half loaded, it would have half the number of ribosomes all clustered at one end of the messenger strand as shown in Fig. 6*b*.

Another possible mechanism is one in which each cistron has its own attachment site so that the ribosomes can initiate the synthesis of proteins on each cistron independently (Fig. 6, top). Thus, for example, when the messenger is half loaded with ribosomes, it may have the appearance seen diagramatically in Fig. 6*a* in which several different proteins are being synthesized at the same time. All of them are partially assembled but none have been completed as yet. In the second type of system, the individual cistrons can be regulated independently so that one cistron may "read out" many times while another one "reads out" only a few times. Of course, it is also possible to imagine mechanisms which combine Figs. 6*a* and 6*b* together.

We have illustrated these two possible idealized "reading" mechanisms because we have used this in interpreting the electron micrographs from the middle and trailing regions of the polio polysome peak. Electron micrographs from position *B* (Fig. 4) in the middle of the polio polysome peak show polysomes with a smaller number of ribosomes attached to them than shown in the leading edge (*A*). However, it is frequently found that gaps appear in the middle of the polysome so that often clusters containing four or five ribosomes will be separated from other clusters by distances of 500 Å or more. Examples are shown in Fig. 7 (*a–c*). In Fig. 7*b* there are seven clusters of ribosomes separated by gaps. This type of gap rarely appears in samples taken from the leading edge (*A*).

The electron micrographs taken from

the trailing edge (*C*) of the polysome distribution shows even greater modification. Here there are fewer ribosomes in the polysomes and they are often widely separated. In this trailing edge, we would expect great heterogeneity, since it might contain viral RNA strands which do not have the full number of ribosomes. Our interest in this regard is the fact that we do not simply observe smaller clusters of ribosomes but rather frequently observe ribosomes which are widely separated from each other. An example is shown in Fig. 7*d* where five ribosomes can be seen attached presumably to an RNA strand, but they are separated by nearly 1000 Å. Several examples of this configuration have been seen in the trailing edge as well as other small clusters of ribosomes which may represent breakdown products associated with sample manipulation.

Because of the great difficulty of preparing samples and because artifacts may arise so easily, clear-cut conclusions cannot be drawn from this type of electron micrograph study. However, this information seems compatible with the type of scheme illustrated in Fig. 6*a* but not entirely compatible with the alternative interpretation in which the ribosome moves along the entire length of the polio RNA strand and repeatedly makes a copy of each protein for which the viral RNA has information. It is clear that the type of mechanism which we are suggesting for polio RNA is capable of a certain amount of control on the polysome level. Thus, for example, it may be possible to produce a small number of copies of the RNA polymerase protein while at the same time producing a large number of copies of the polio-coat protein. There are some indications that a control mechanism exists for polio virus production since approximately half the C^{14} amino acids in infected, actinomycin-D treated HeLa cells are found in virus-coat protein (*9*). Other systems of polycistronic reading mechanisms have also been discussed recently (*13*).

Our observations and interpretations may be regarded as tentative; they do not establish a mechanism for the polio virus polycistronic messenger RNA, but they may stimulate further experimentation (*14*).

ALEXANDER RICH, SHELDON PENMAN
YECHIEL BECKER, JAMES DARNELL
CECIL HALL
Department of Biology, Massachusetts Institute of Technology, Cambridge

References and Notes

1. J. R. Warner, A. Rich, C. E. Hall, *Science* **138**, 1399 (1962).
2. J. R. Warner, P. M. Knopf, A. Rich, *Proc. Natl. Acad. Sci. U.S.* **49**, 122 (1963).
3. A. Gierer, *J. Mol. Biol.* **6**, 148 (1963); F. O. Wettstein, T. Staehlin, H. Noll, *Nature* **197**, 430 (1963).
4. S. Penman, K. Scherrer, Y. Becker, J. Darnell, *Proc. Natl. Acad. Sci. U.S.* **49**, 654 (1963).
5. M. D. Scharff, A. J. Shatkin, L. Levintow, *ibid*, **50**, 686 (1963).
6. Equipment: Dounce homogenizer; SW25, Spino model L ultracentrifuge; Guilford spectrometer; RCA EMU-3 electron microscope.
7. H. Slayter, J. R. Warner, A. Rich, C. E. Hall, *J. Mol. Biol.*, in press.
8. H. Goodman and A. Rich, *Nature* **199**, 318 (1963).
9. S. Penman, Y. Becker, J. Darnell, in preparation.
10. J. T. Finch and A. King, *Nature* **183**, 1709 (1959).
11. J. Maizel, in press.
12. D. Baltimore, H. J. Eggers, R. M. Franklin, I. Tamm, *Proc. Natl. Acad. Sci. U.S.* **49**, 843 (1963).
13. *Cold Spring Harbor Symp.* **27** (1963).
14. Supported by grants from the U.S. Public Health Service and the National Science Foundation.

18 November 1963

Nitrogen and Potassium Effect on the Color of Red Roses

Abstract. *Variable coloration was displayed by* Rosa hybrida, *var. Better Times, grown in solutions of various concentrations of nitrogen and potassium. As revealed by measuring the color in Hunter values, growth in high potassium and low nitrogen concentrations resulted in less reddish and more bluish roses, while cultivation in a low nitrogen concentration, irrespective of the N/K ratio, resulted in roses which were more lightly colored than those grown in high concentrations of nitrogen and potassium. The results were statistically significant at the 1 percent probability level.*

The chief pigment of red roses is the anthocyanin, cyanidin 3,5-diglucoside (*1*). The color of plant tissues pigmented with anthocyanins is affected by a number of factors, such as the concentration and association of these pigments with other substances, the *p*H, the ash content and colloidal state of the cell sap, the nature and concentration of other pigments, and so forth (*2*).

The nutritional state of the plant has also been connected with the color of anthocyanin-pigmented tissues (*3*). Red roses tend to turn paler owing to inadequate carbohydrate supplies (*4*), and an excess of potassium in relation to nitrogen in the growth medium imparts a bluish hue to the petals (*5*).

The object of this study was to assess the effect of certain levels of potassium and nitrogen available to the plant on the color of red roses, and to use instrumental methods of color evaluation rather than visual observation.

Nonrooted rose cuttings of *Rosa hybrida*, var. Better Times, were placed in moist sand and after rooting they were transferred to glazed crocks filled with No. 7 AGSAE Flint quartz sand. Growth was initiated in a standard Hoagland solution. The sand was then washed with distilled water and nutrient solutions representing four combinations of two concentrations of N and K were applied. The two concentrations of these elements differed by a factor of three (Table 1). The nutrient solutions were applied twice a day to the surface of the sand and the excess solution was collected in containers kept below the crocks. The nutrient solutions were made fresh weekly.

The roses were cut 4 days after opening and six petals were detached from the two outermost rows of each rose. The color of each petal was measured individually with the Gardner color difference meter. The petal was placed between the two plates of a petri dish (the smaller plate was blackened and inverted) with the centers of the light spot and the petal made to coincide. Evaluation of the color was made in terms of the Hunter values L, a_L, and b_L. The instrument was calibrated with standard tile B44, L 24.8, a_L +20.4, b_L = +6.0 (*6*).

This method of measuring the color of roses was considerably more sensitive than either the comparison of the absorption spectra of extracts and expressed sap of the petals or the comparison of the reflectance spectra of the petals by means of a Beckman DU spectrophotometer.

Table 1. Composition of nutrient solutions (grams/liter). In addition, the solutions contained magnesium sulfate, the iron salt of EDTA, and trace elements.

1N-1K	1N-3K	3N-1K	3N-3K
	$Ca(NO_3)_2 \cdot 4H_2O$		
0.4723	0.4723	0.4723	0.4723
	$NH_4H_2PO_4$		
0.1726	0.1726	0.1726	0.1726
	NH_4NO_3		
0.0160	0.0160	1.0086	0.5436
	KNO_3		
0.6571	0.6571	0.6571	1.8196
	KH_2PO_4		
0.1361	0.1361	0.1361	0.1361
	KCl		
0.07455	1.3419	0.07455	0.4848